REPORT ON TWO TOPICS: RELATIONSHIP BETWEEN THE DUST AND WATER CYCLES IN THE GCM / DUST DEVILS AT PATHFINDER.

S. M. Nelli, *New Mexico State University, Las Cruces, NM (snelli@nmsu.edu),* **J. R. Murphy**, *Department of Astronomy, New Mexico State University, Las Cruces, NM, USA (murphy@nmsu.edu).*

Relationship between the dust and water cycles in the GCM.

Introduction:

Mars' atmosphere is carbon dioxide dominated with non-negligible amounts of water vapor and suspended dust particles. The atmospheric dust plays an important role in the heating and cooling of the planet through absorption and emission of radiation. Small dust particles can potentially be carried to great altitudes and affect the temperatures there. Water vapor condensing onto the dust grains can affect the radiative properties of both, as well as their vertical extent. The condensation of water onto a dust grain will change the grain's fall speed and diminish the possibility of dust obtaining high altitudes. In this capacity, water becomes a controlling agent with regard to the vertical distribution of dust. Similarly, the atmosphere's water vapor holding capacity is affected by the amount of dust in the atmosphere. Dust is an excellent green house catalyst; it raises the temperature of the atmosphere, and thus, its water vapor holding capacity. There is, therefore, a potentially significant interplay between the Martian dust and water cycles.

Previous research done using computer modeling to better understand the Martian atmosphere treat the dust and the water cycles as two separate and independent processes. The existing numerical model will be improved to simulate the relationship between the Martian dust and water cycles by actually coupling the two cycles. The model will condense the water onto the dust allowing the particle's radiative characteristics, fall speeds, and as a result, their vertical distribution to change. Data obtained from the Viking, Mars Pathfinder, and especially the Mars Global Surveyor missions will be used to determine the accuracy of the model results.

Discussion:

The water and dust cycles in the model will be coupled by freezing supersaturated water vapor onto the dust grains to form clouds. By using the dust as seeds for cloud formation, the radiative properties, fall speeds and vertical distributions of both will be altered [1,2]. Water ice encapsulating the dust grains makes the dust much less effective at the 15µm absorption band, but increases their potential as infrared scatterers [2]. Mie scattering (the scattering of light by a particle whose size is comparable to the wavelength of light) becomes important with the formation of cloud particles a few microns in size. The effectiveness of Mie scattering is large when the size parameter, $2\pi r/\lambda \geq 1$, where r is the radius of the particle and λ is the wavelength of light.

The addition of water mass to these dust grains influences the gravitational sedimentation speed. First, the increase in mass decreases the sedimentation speed, and then the fall speed rapidly increases once the particle has doubled in radius, removing dust more quickly from the atmosphere [3]. The vertical extent of the dust will be at the mercy of the cloud deck. Little, if any, dust will be able to be transported past the saturation layer. Here, the dust will be used for seeds in cloud formation, effectively capping its altitude. The "snowing out" of these particles will move water out of the saturated layer to lower vertical levels as well.

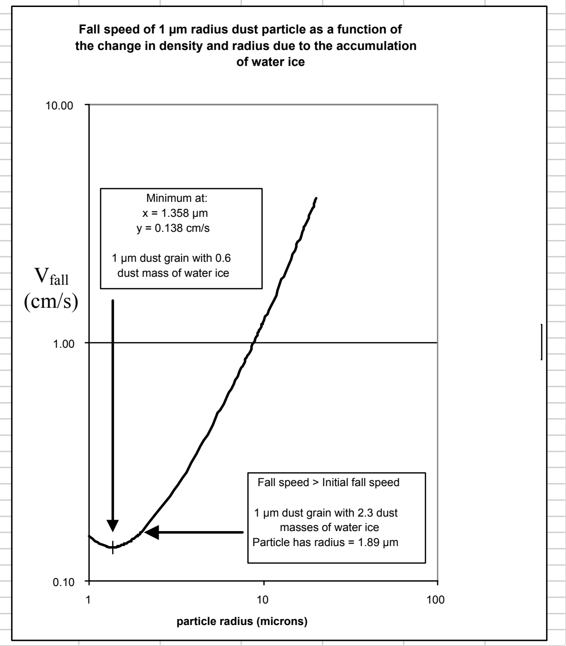

Sublimation of ground ice is based upon the flux rate equations of Haberle and Jakosky [4] for buoyant diffusion (E_b) and turbulent mixing (E_t). These two processes are as follows:

$$E_b = (0.17)(\delta\eta)\rho D[(\delta\rho/\rho)(g/\nu^2)]^{1/3}$$

and

$$E_t = (0.002)\rho w q_s(1 - r)$$

where δη is the difference between the surface concentration (by mass) of water vapor and that of the gas away from the surface, ρ is the density of the atmosphere, D is the diffusion coefficient of water vapor in CO_2, g is the acceleration due to gravity, ν is the kinematic viscosity of CO_2, δρ is the difference between the density of the atmosphere at the surface and the density of water vapor at the surface, *w* is the wind speed at the surface layer, q_s is the saturation mixing ratio of water vapor at the temperature of the ice, and r is the relative humidity [4].

The model will contain an adsorbing regolith based on the scheme developed by Houben et al. [5]. Water will be mobilized in an approximately 10 cm thick ground layer. The total adsorbed water capacity is by:

$$\alpha = \varepsilon\rho_s[\beta P^{0.51}{}_{H2O}/\exp(\delta/T)]$$

where ρ_s is the density of the regolith, β is the specific soil surface area for basalt, δ = -2679.8 K, T is the temperature, P_{H2O} is the water vapor pressure in Pascals, and ε is a dimensionless parameter introduced to allow for scaling the adsorptive properties of other minerals. Increasing the value of ε will increase the adsorptivity of the soil, meaning the regolith can hold more water per unit volume [5].

The exact parameters for cloud formation have not yet been determined. There are several questions that the authors are currently answering. What percentage of supersaturation will go into cloud formation? What size cloud particle(s) to form? What "sticking" parameter do we use (or, how do we go about making the cloud particles)? We intend to look at global scales, therefore, microphysical calculations are not prudent. We wish to make a ten's of years simulation, and do not want the model to run in real time. Initial answers to these questions will be given at the conference for criticism.

References:

[1] Rodin et al. (1999) *Advances in Space Science*, 23, 1577-1585. [2] Clancy et al. (1998) AAS, DPS meeting #30, Abstract #09.02. [3] Murphy et al. (1990) *JGR*, 95, 14629-14648. [4] Haberle R.M. & Jakosky B.M. (1990) *JGR*, 95, 1423-1437. [5] Houben et al. (1997) *JGR*, 102, 9069-9083.

Dust devils at Pathfinder.

Introduction:

Over the course of its 83 sol mission, the Mars Pathfinder lander detected the presence of 79 small-scale convective vortices. When accounting for the incompleteness of the data set (the pressure sensor was not turned on continuously), one can infer that at least two vortices passed by the lander each sol. The diurnal variation of these vortices is similar to that of terrestrial dust devils. If the horizontal wind of these vortices reach speeds capable of lifting dust, then their frequency of occurrence allows for the maintaining of atmospheric dust loads against sedimentation. The local frequency of occurrence from the Pathfinder data set can be combined with the regional frequency of occurrence obtained from orbiter images to potentially quantify the effect small-scale vortices have on the atmospheric dust cycle.

Vortex Occurrence Determination:

Identification of small-scale convective vortices was based on the measurement of the surface pressure taken by the Mars Pathfinder lander Atmospheric Structure Investigation/Meteorology (ASI/MET) experiment. Specifically, we looked for an abrupt drop in the measured surface pressure, followed by an equally abrupt rise in the measured surface pressure. An increase in temperature from warm-core vortices [6] and rapid variation in wind direction can also be indicative of a passing vortex. However, we did not use the temperature or wind data sets in our analysis. The turbulent nature of the near-surface environment can cause the temperature and wind direction to vary wildly without the presence of a passing vortex. Hence, the temperature and wind direction are not always diagnostic.

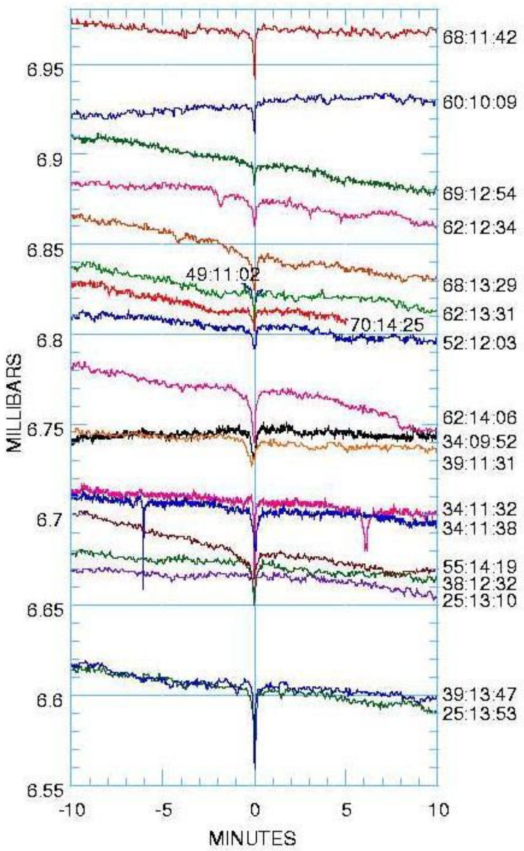

Figure 1. Plotted time series of measured Mars Pathfinder surface pressure illustrating the pressure signatures of nineteen separate small-scale convective vortices passing by the northern-subtropical landing site during the 83 sols of the mission. Times along the right vertical axis (sol:hour:minute) represent the local true solar time of the vortex pressure minimum. The maximum observed vortex depression was 0.0477 millibars (4.77 Pascals) at 11:32 on sol 34.

The Pathfinder data set for the 83 sol mission was divided into 15-minute intervals. A 3rd order polynomial was fit to each 15-minute interval of data and the difference between the two was taken. After calculating the mean of the difference, any instantaneous difference greater than three standard deviations from the mean and whose absolute difference was ≥0.005 millibars was tagged for closer inspection. One hundred and twenty-five instances were tagged. Visual analysis lead to the identification of 79 vortex occurrences. False detections occurred due to internal gaps in the data.

The 79 occurrences average to one detection per sol by the lander. However, on the five days in which the ASI/MET experiment ran continuously, an average 4.2 vortices per sol were detected by the lander. All detections of vortices occurred from 9:30-17:00 local time. On twenty-one days, there were multiple detections of vortices at the lander site. Early afternoon was the peak for observed vortex occurrence. This dependence is consistent with terrestrial analogs [7].

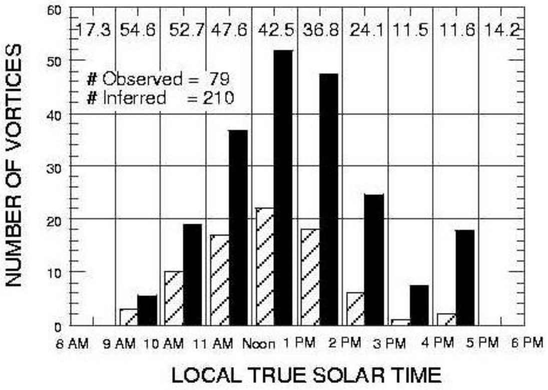

Figure 2. Time-of-sol occurrence (binned in to hourly segments) of convective vortices at the Mars Pathfinder site. Grey indicators represent actual observed vortex occurrence. Black indicators represent the 'inferred' number of vortex occurrences obtained via normalization of the observed numbers by the data fractional temporal coverage. Fractional temporal coverage (multiplied by 100) within each hour is indicated by the numeric values located just below the top axis within each hour interval.

Sampling was incomplete because the meteorological package did not operate continuously. We account for this incompleteness by deriving an inferred vortex occurrence value. We calculated the total minutes of coverage in each 15-minute interval over the 83 sol mission and normalized this to the total possible time coverage in that interval for 83 sols (83 sols x 15 minutes per sol = 1245 minutes). We then normalized the accumulated number of vortices observed in a 15-minute interval by the fraction of time covered for that interval. Figure 2 shows our normalization summed over one-hour intervals. Our normalization suggests 210 vortices passed by the lander during the 83 sols of the mission, an average of ~2.5 per day.

Discussion:

Taking into consideration the frequency of occurrence generated above and inferences of dust devil occurrence by orbital imaging, one can strongly suggest that small-scale convective vortices are omnipresent on Mars. Because suspended dust is thermodynamically active, small-scale convective vortices become important when their wind speeds are capable of lifting dust. Dust devils can become an important contributing factor when larger scale dust lifting does not dominate (northern summer, [8]). Below we quantify the effect dust devils can have on the local atmospheric dust content based on the frequency of occurrence inferred from the Mars Pathfinder lander data set.

Mars Pathfinder Imager (IMP) captured five dust devil occurrences during the second ten sols of the mission [9]. These vortices possessed diameters of 14-79 meters, heights of 46-350 meters, and dust concentration of $7\text{x}10^{-5}$ kg m^{-3}. A dust devil of average dimension (diameter = 50 m, height = 250 m, dust concentration = $7\text{x}10^{-5}$ kg m^{-3}) would carry an instantaneous dust load of 134 kg. If spread over a 1.5 km diameter in the sky, an optical depth increase of 0.01 would occur. Since dust devils are not static, dust cycles through the vortex continuously, causing the above estimate to be conservative.

If assuming an exponential decay similar to that seen at the end of the 1977B global dust storm [10], a rate for the decline of optical depth can be calculated:

$$\Delta_\tau = \tau_{rmO} \times (1 - \exp[-t/75]) = 0.007 \text{ for } \tau_O = 0.5 \text{ and } t = 1 \text{ sol}$$

Note, the optical depth decay rate ($\Delta_\tau = 0.007$) is comparable to the upward dust devil flux ($\Delta_\tau = 0.01$). One can estimate the upward flux of dust by convective vortices on a regional scale by inferring a frequency of occurrence from orbiter images. In the future, a global application of lander derived diurnal variation versus orbiter determined spatial coverage may become reality, but that will require a network of landed stations.

References:

[6] Renno et al. (2000) *JGR*, 105, 1859-1865. [7] Sinclair P.C. (1969) *J. Appl. Meteor.*, 8, 32-45. [8] Murphy J.R. (1999) 5th International Conference on Mars, Abstract #6087, LPI Contribution 972. [9] Metzger et al. (1999) GRL, 26, 2731-2734. [10] Pollack et al. (1979) *JGR*, 84, 2929-2945.